11

Modeling, Motion Planning and Control of the Drones with Revolving Aerofoils: an Outline of the XSF Project*

Lotfi Beji[1], Azgal Abichou[2], and Naoufel Azouz[1]

[1] LSC Laboratory, CNRS-FRE2494, Université d'Evry Val d'Essonne. 40, rue du Pelvoux, 91020, Evry Cedex, France {beji|azouz}@iup.univ-evry.fr
[2] LIM Laboratory, Ecole Polytechnique de Tunisie, BP 743, 2078 La Marsa, Tunisia azgal.abichou@ept.rnu.tn

11.1 Introduction

Aerial robotics has been known for several years as a considerable passion of private manufacturers as well as research laboratories. This interest is justified by the recent technological projections which make possible the design of powerful systems endowed with real capacities of autonomous navigation, at non-prohibitive cost. Today, the principal limitations which the researchers meet are related on one hand to the difficulty of controlling the apparatus in the presence of atmospheric turbulences, and on the other hand to the complexity of the problem of navigation requiring the perception of often constrained and evolutionary environment, in particular in the case of flights at low altitude. The applications are numerous. They initially relate to areas of safety (monitoring the airspace, urban and interurban traffic), natural risk management (monitoring the activity of volcanoes), environmental protection (measurement of the air pollution, monitoring the forests), intervention in hostile sites (radioactive media, mine clearance of the grounds without human intervention), management of large infrastructures (stoppings, high-voltage lines, pipelines), agriculture (detection and treatment of the cultures) and the catch of air sight in the production of films. All these missions require a powerful control of the apparatus and consequently precise information on its absolute and/or relative state with respect to its environment. Contrary to terrestrial mobile robots for which it is often possible to be limited to a kinematic model, control of aerial robots requires the knowledge of a dynamic model. The effects of gravity and the aerodynamic loads are the principal causes. These systems, for which the number of control inputs is lower than the number of degrees of freedom, are known as underactuated. The mechanism of control provides generally only one or two inputs for the translational dynamics and two or three inputs for the rotational dynamics. At the beginning of the nineties, the automation community

* This work is supported by the mini-flyer competition program organized by the DGA (Direction Générale des Armements) and the ONERA (Office Nationale d'Etude et de Recherche en Aérospatiale), France.

K. Kozłowski (Ed.): Robot Motion and Control, LNCIS 335, pp. 165–177, 2006.

showed a renewal of interest in control of these systems. An outstanding example is a thorough study carried out on the dynamics of planes like VTOL (Vertical Take-Off and Landing) which made it possible to constitute an important source of knowledge and led to additional developments on the flat system theory and the techniques of linearization input-outputs [1, 2].

More recently, several researchers serve of their experiment on control mobile robots moving on the ground, in cooperation with control of flying machines.

Modelling and controlling aerial vehicles (blimps, mini rotorcraft) are the principal preoccupation of the *Lsc*, *Lim*-groups. Competition of the DGA-ONERA program won the XSF project which consists of a drone with revolving aerofoils. It is equipped with four rotors where two are directionals, what we call in the text *bidirectional* X4-flyer. In fact, the study of quad-rotor vehicles is not recent. However, combination of revolving aerofoils and directional rotors were attractive for the contest. In this topic, a mini-UAV was constructed by the *Lsc*-group taking into account industrial constraints. The aerial flying engine couldn't exceed 2 kg in mass, and 70 cm of scale with approximatively 30 min of flying-time. Compared to helicopters, named quad-rotor [3], the four-rotor rotorcraft has some advantages [4, 5]: given that two motors rotate counter clockwise while the other two rotate clockwise, gyroscopic effects and aerodynamic torques tend, in trimmed flight, to cancel. Vertical motion is controlled by collectively increasing or decreasing the power for all motors.

In a conventional X4-flyer, the longitudinal/lateral motion in x/y direction is achieved by differentially controlling the motors generating a pitching/rolling motion of the airframe that inclines the thrust (producing horizontal forces) and leads to lateral accelerations. In a bidirectional X4 flyer, without generating rotation of the engine, we can only rotate two rotors with respect to their local frame and have lateral motions. The motion planing and control of these configurations are new. With respect to the literature, we cite the VTOL stabilization by Hamel [5], where the dynamic motor effects are incorporated. The robust output regulation for autonomous vertical landing was studied by Marconi [8]. The stabilization results for the X4-flyer by the nested saturation algorithm were given by Castillo [6]. That work was illustrated by successful tests. In the case of the PVTOL (Planar), the stabilization was solved with the input/output linearization procedure [7] and the theory of flat systems [1, 2]. As we can see, the control of flying vehicles is limited to the stabilization problem. In this work, tracking results are presented.

This article is organized in the following way: Section 11.2 describes the worked out translational and rotational motions. Section 11.3 presents the developed ideas of control for the conventional X4-flyer and the bidirectional one. A strategy to solve the tracking problem through point to point steering is shown in Section 11.4. The simulation tests, results, comments and the prospects for evolution of research conclude the work.

11.2 Configuration Description and Modeling

The conventional and the bidirectional XSF are systems consisting of four individual electrical fans attached to a rigid cross frame. We consider a local reference airframe $\Re_G = \{G, E_1^g, E_2^g, E_3^g\}$ at G (mass center), while the inertial frame is $\Re_o = \{O, E_x, E_y, E_z\}$ such that the vertical direction E_z is upwards. Let the vector

$X = (x, y, z)$ denote the G position with respect to $\Re_o$. The rotation of the rigid body is defined by $R_{\phi,\theta,\psi} : \Re_o \rightarrow \Re_G$, where $R_{\phi,\theta,\psi} \in SO(3)$ is an orthogonal rotation matrix which is defined by the Euler angles, θ(pitch), ϕ(roll) and ψ(yaw), regrouped in $\eta = (\phi, \theta, \psi)$. A conceptual form is sketched in Fig. 11.1.

The XSF is a quadrotor of 68 cm × 68 cm of total size. It is designed in a cross form and made of carbon fiber. Each tip of the cross has a rotor including an electric brushless motor, a speed controller and a two-blade ducted propeller. In the middle one can find a central cylinder enclosing electronics, namely Inertial Measurement Unit, on-board processor, GPS, radio transmitter, cameras and ultrasound sensors, as well as the LI-POLY batteries. The operating principle of the XSF can be presented as follows: two rotors turn clockwise, and the other two rotors turn counter-clockwise to maintain the total equilibrium in yaw motion. With the equilibrium of the angular velocities of all the rotors maintained, the XSF is either in a fixed position, or moving vertically (changing altitude). A characteristic of the XSF compared to other quadrotors is the swiveling of the supports of the motors 1 and 3 around the pitching axis due to two small servomotors (Fig. 11.2). This permits a more stabilized horizontal flight and a suitable cornering.

Fig. 11.1. Conceptual form of the X4 Super-Flyer (XSF)

11.3 Aerodynamic Forces and Torques

In this part we will define the characteristics of the aerodynamic forces and torques resulting from the blade theory. The blade behaves as a rotating wing. Each element of the blade dr is in contact with the airflow with a speed V_R and according to an angle of attack α. One call pans the axisymmetric hooding of the hub, interdependent of the propeller in rotation. In the plan of the propeller, the pan is defined by the radius R_o.

Each elementary section of the blade of width dr creates a lift dL and a drag dD [9], such as

$$dL = \frac{1}{2}\rho C_L V_R^2 dS, \qquad dD = \frac{1}{2}\rho C_D V_R^2 dS, \tag{11.1}$$

where ρ is the air density, C_L and C_D represent adimensional coefficients of lift and drag depending mainly on the angle of attack α ($\alpha = \gamma - \Phi$, see Fig. 11.3). According

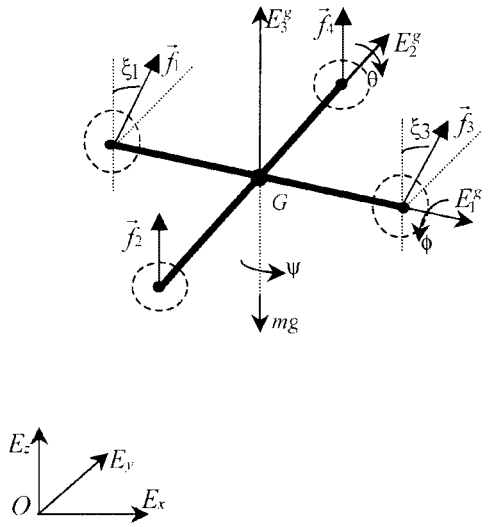

Fig. 11.2. Frames attached to the X4 bidirectional rotors rotorcraft

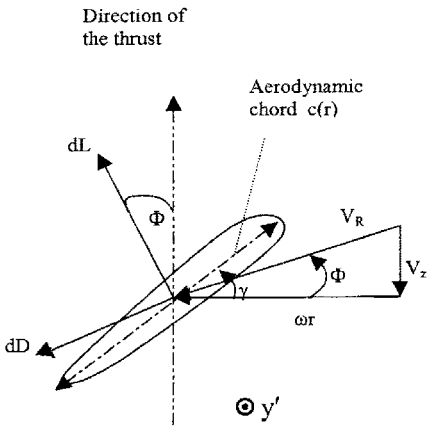

Fig. 11.3. Description of forces applied to the blade

to the fact that the XSF will hover or move at low speed, we made the assumption that the thrust f for a B blades propeller can be written as:

$$f = \frac{B}{2}\rho \int_{R_0}^{R} V_R^2 c(r) C_L(r) dr = \frac{B}{2}\rho\omega^2 \int_{R_0}^{R} r^2 c(r) C_L(r) dr. \tag{11.2}$$

We can eliminate this sentence which seems to be unclear or not necessary. Then the paragraph becomes:

$$f = K_T \omega^2. \tag{11.3}$$

The computation of the lift coefficient is often complex. It is thus essential to elaborate an experimental process, which permits to determine precisely the coefficient K_T as well as the limits of validity of the relation.

The drag torque is defined similarly as

$$M_D = \frac{B}{2}\rho \int_{R_0}^{R} V_R^2 c(r) C_D(r) r dr = \frac{B}{2}\rho\omega^2 \int_{R_0}^{R} c(r) C_D(r) r^3 dr \tag{11.4}$$

or simply

$$M_D = K_M \omega^2. \tag{11.5}$$

The compensation of this torque in the center of gravity is established thanks to the use of contrarotating rotors 1-3 and 2-4. Recall that rotors 2 and 4 turn counterclockwise while rotors 1 and 3 turn clockwise.

11.4 Dynamics of Motion

We consider the translation motion of $\Re_G$ with respect to (*wrt*) $\Re_o$. The position of the mass center *wrt* $\Re_o$ is defined by $\overrightarrow{OG} = (x\ y\ z)^T$, its time derivative gives the velocity *wrt* to $\Re_o$ such that $\frac{d\overrightarrow{OG}}{dt} = (\dot{x}\ \dot{y}\ \dot{z})^T$, while the second time derivative permits to get the acceleration: $\frac{d^2\overrightarrow{OG}}{dt^2} = (\ddot{x}\ \ddot{y}\ \ddot{z})^T$:

$$\begin{aligned} m\ddot{x} =& S_\psi C_\theta u_2 - S_\theta u_3, \\ m\ddot{y} =& (S_\theta S_\psi S\phi + C_\psi C\phi) u_2 + C_\theta S_\phi u_3, \\ m\ddot{z} =& (S_\theta S_\psi C\phi - C_\psi S\phi) u_2 + C_\theta C_\phi u_3 - mg, \end{aligned} \tag{11.6}$$

where m is the total mass of the vehicle. The vector u_i, $i = 2, 3$ combines the principal non conservative forces applied to the X4 bidirectional flyer airframe including forces generated by the motors and drag terms. Recall that the aerodynamic drag force is given by the classical relation : $F_D = \frac{1}{2}\rho_{air} V^2 S C_D$, where S is a reference area, C_D is the drag coefficient of the quadrotor in forward flight. We assume here that the apparent speed V of the XSF is small (< 4 m/s), thus we neglect force F_D in the dynamic model. Gyroscopic torques due to motors effects can be also neglected.

The lift (collective) force u_3 and the directional force u_2 are such that

$$\begin{pmatrix} 0 \\ u_2 \\ u_3 \end{pmatrix} = f_1 e_1' + f_3 e_3' + f_2 e_2 + f_4 e_4 \tag{11.7}$$

with $f_i = K_T \omega_i^2$, $K_T > 0$ and constant (more details about K_T are given in Section 11.3), ω_i is the angular speed of motor i. In the local frame $\Re_G$ it is straightforward to verify that

$$e_1' = \begin{pmatrix} 0 \\ S_{\xi 1} \\ C_{\xi 1} \end{pmatrix}_{\Re_G}, \quad e_3' = \begin{pmatrix} 0 \\ S_{\xi 3} \\ C_{\xi 3} \end{pmatrix}_{\Re_G}, \quad e_2 = e_4 = \begin{pmatrix} 0 \\ 0 \\ 1 \end{pmatrix}_{\Re_G}.$$

Then we can write

$$\begin{aligned} u_2 &= f_1 S_{\xi 1} + f_3 S_{\xi 3}, \\ u_3 &= f_1 C_{\xi 1} + f_3 C_{\xi 3} + f_2 + f_4, \end{aligned} \tag{11.8}$$

where ξ_1 and ξ_3 are the two internal degrees of freedom of rotors 1 and 3, respectively. These bounded variables are controlled by DC servo-motors. e_2 and e_4 are the unit vectors along E_3^g which imply that rotors 2 and 4 are identical to that of the conventional X4-flyer. According to classical mechanics, the rotational dynamics is as follows:

$$\begin{aligned} \ddot{\theta} &= \frac{1}{I_{xx} C_\phi} (\tau_\theta + I_{xx} S_\phi \dot{\phi} \dot{\theta}), \\ \ddot{\phi} &= \frac{1}{I_{yy} C_\phi C_\theta} (\tau_\phi + I_{yy} S_\phi C_\theta \dot{\phi}^2 + I_{yy} S_\theta C_\phi \dot{\theta} \dot{\phi}), \\ \ddot{\psi} &= \frac{1}{I_{zz}} \tau_\psi, \end{aligned} \tag{11.9}$$

where the inertia matrix $I_G = \mathrm{diag}(I_{xx}, I_{yy}, I_{zz})$, and the three inputs in torque

$$\begin{aligned} \tau_\phi &= l(f_2 - f_4), \\ \tau_\theta &= l(f_3 C_{\xi 3} - f_1 C_{\xi 1}), \\ \tau_\psi &= l(f_3 S_{\xi 3} - f_1 S_{\xi 1}) + \frac{K_M}{K_T} (f_3 C_{\xi 3} - f_1 C_{\xi 1} + f_4 - f_2), \end{aligned} \tag{11.10}$$

where l is the distance from G to the rotor i. Note that $\tau_\psi = \frac{K_M}{K_T}(f_3 - f_1 + f_4 - f_2)$, which is the case of the conventional machine ($\xi_1 = \xi_3 = 0$). Then with the bidirectional rotors, more manoeuver is obtained in yaw motion.

The equality from (11.9) is ensured, meaning that

$$\ddot{\eta} = \Pi_G(\eta)^{-1} (\tau - \dot{\Pi}_G(\eta) \dot{\eta}) \tag{11.11}$$

with $\tau = (\tau_\theta \ \tau_\phi \ \tau_\psi)^T$ as an auxiliary input, and

$$\Pi_G(\eta) = \begin{pmatrix} I_{xx} C_\phi & 0 & 0 \\ 0 & I_{yy} C_\phi C_\theta & 0 \\ 0 & 0 & I_{zz} \end{pmatrix}. \tag{11.12}$$

As a first step, the model given above can be input/output linearized by the following decoupling feedback laws

$$\begin{aligned} \tau_\theta &= -I_{xx} S_\phi \dot{\phi} \dot{\theta} + I_{xx} C_\phi \tilde{\tau}_\theta, \\ \tau_\phi &= -I_{yy} S_\phi C_\theta \dot{\phi}^2 - I_{yy} S_\theta C_\phi \dot{\theta} \dot{\phi} + I_{yy} C_\phi C_\theta \tilde{\tau}_\phi, \\ \tau_\psi &= I_{zz} \tilde{\tau}_\psi \end{aligned} \tag{11.13}$$

and the decoupled dynamic model of rotation can be written as

$$\ddot{\eta} = \tilde{\tau} \tag{11.14}$$

with $\tilde{\tau} = (\tilde{\tau}_\theta \ \tilde{\tau}_\phi \ \tilde{\tau}_\psi)^T$. Using the system of Equations (11.6) and (11.14), the dynamics of the system is defined by

$$\begin{aligned} m\ddot{x} &= S_\psi C_\theta u_2 - S_\theta u_3, \\ m\ddot{y} &= (S_\theta S_\psi S_\phi + C_\psi C_\phi) u_2 + C_\theta S_\phi u_3, \\ m\ddot{z} &= (S_\theta S_\psi C_\phi - C_\psi S_\phi) u_2 + C_\theta C_\phi u_3 - mg, \\ \ddot{\theta} &= \tilde{\tau}_\theta, \qquad \ddot{\phi} = \tilde{\tau}_\phi, \qquad \ddot{\psi} = \tilde{\tau}_\psi. \end{aligned} \tag{11.15}$$

Remark 1. As shown in (11.15), the equivalent system of the control-inputs presents five inputs $U = (u_2, u_3, \tilde{\tau}_\theta, \tilde{\tau}_\phi, \tilde{\tau}_\psi)$, while the rotor force-inputs are of sixth order (see relations 11.7,11.10) $F = (f_1, f_2, f_3, f_4, \xi_1, \xi_3)$. Then the transformation $U \mapsto F$ is not a diffeomorphism.

11.4.1 Dynamic Motion of the Conventional X4 Flyer

One deduces this dynamic after substituting $\xi_1 = \xi_3 = 0$ in Eqs. (11.15) and (11.8):

$$\begin{aligned} m\ddot{x} &= -S_\theta u_3, \\ m\ddot{y} &= C_\theta S_\phi u_3, \\ m\ddot{z} &= C_\theta C_\phi u_3 - mg, \\ \ddot{\theta} &= \tilde{\tau}_\theta, \qquad \ddot{\phi} = \tilde{\tau}_\phi, \qquad \ddot{\psi} = \tilde{\tau}_\psi. \end{aligned} \tag{11.16}$$

Remark 2. In the conventional X4-flyer (see Fig. 11.4, right) case, where we consider $\xi_1 = \xi_3 = 0$, the yaw motion is generated by $\tau_\psi = \frac{K_M}{K_T}(f_1 - f_2 + f_3 - f_4)$. The collective input in (11.16) is given by $u_3 = f_1 + f_3 + f_2 + f_4$.

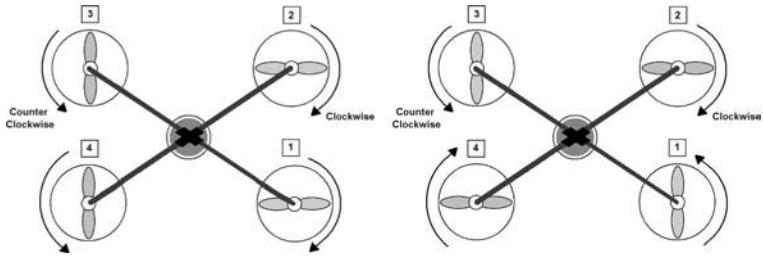

Fig. 11.4. Rotor rotations: bidirectional (left) and conventional (right)

11.5 Advanced Strategies of Control

Our aim in the XSF project is to test the capability of the drone while progressing in an area with approximatively ten-meter buildings. In this part, we will present briefly the point-to-point based tracking of the conventional X4-flyer. The reader can refer to Beji [10] for more details. More attention will be given to the bidirectional engine which was also studied by Beji [11] but not compared to the conventional one.

11.5.1 Conventional Aerial Vehicle

The tracking control problem was solved using the point-to-point steering. For the tracking problem, each point will be stabilized and tracked as a starting one. Flatness was proved with respect to the flat output (x, y, z) [10]. Recall that a system is flat

if we can find a set of outputs (equal in number to the number of inputs) such that all states and inputs can be determined from these outputs without integration [2].

We proved that the state and the control vector are function of the flat output and their time derivatives. For a given smooth trajectory $\xi(t)=(x(t), y(t), z(t))$. We get $(u_3 > 0)$

$$\begin{aligned} u_3 &= m\left(\ddot{x}^2 + \ddot{y}^2 + (\ddot{z}+g)^2\right)^{\frac{1}{2}}, \\ \phi &= \arctan\left(\frac{\ddot{y}}{\ddot{z}+g}\right) \quad \text{and} \quad \theta = -\arctan\left(\frac{c_\phi \ddot{x}}{\ddot{z}+g}\right). \end{aligned} \tag{11.17}$$

Indeed, u_3, θ, ϕ, $\dot{u}_3$, $\dot{\theta}$, and $\dot{\phi}$ are functions of $\ddot{\xi}, \xi^{(3)}$. Thus it is straightforward to verify that states and inputs are functions of $(\xi, \dot{\xi}, \xi^{(2)}, \xi^{(3)})$. Moreover, we can derive $\theta(t)$, $\phi(t)$ and prove the ξ-dependency of $\tilde{\tau}_\theta$ and $\tilde{\tau}_\phi$ as function of $(\xi^{(2)}, \xi^{(3)}, \xi^{(4)})$.

From Eq. (11.16), the yaw motion can be naturally stabilized to a desired value (second order with constant coefficients) and the z altitude can be stabilized by u_3 (nonlinear decoupling feedback). The results are regrouped in the following theorem.

Theorem 1. *Consider the dynamics of the conventional aerial vehicle given by (11.16). The following control inputs stabilize any desired configuration* $(x_d, y_d, z_d, \psi_d, \theta_d, \phi_d)$, *where* $\psi_d = n\pi$, $\theta_d \in [\theta_d^m, \theta_d^M]$ *and* $\phi_d \in [\phi_d^m, \phi_d^M]$:

$$\begin{aligned} u_3 &= mg + m\ddot{z}_d - mk_1^z(\dot{z}-\dot{z}_d) - mk_2^z(z-z_d), \\ \tilde{\tau}_\psi &= \ddot{\psi}_d - k_1^\psi(\dot{\psi}-\dot{\psi}_d) - k_2^\psi(\psi-\psi_d), \\ \tilde{\tau}_\theta &= -\frac{1}{g+f(z,z_d)}(\nu_x + \ddot{f}(z,z_d)\theta + 2\dot{f}(z,z_d)\dot{\theta}), \\ \tilde{\tau}_\phi &= -\frac{1}{g+f(z,z_d)}(\nu_y + \ddot{f}(z,z_d)\phi + 2\dot{f}(z,z_d)\dot{\phi}), \\ \nu_x &= x_d^{(4)} - k_1^x(x^{(3)} - x_d^{(3)}) - k_2^x(\ddot{x}-\ddot{x}_d) - k_3^x(\dot{x}-\dot{x}_d) - k_4^x(x-x_d), \\ \nu_y &= y_d^{(4)} - k_1^y(y^{(3)} - y_d^{(3)}) - k_2^y(\ddot{y}-\ddot{y}_d) - k_3^y(\dot{y}-\dot{y}_d) - k_4^y(y-y_d). \end{aligned} \tag{11.18}$$

Here, the function $f(z,z_d) = \ddot{z}_d - k_1^z(\dot{z}-\dot{z}_d) - k_2^z(z-z_d)$ *is assumed to be regular wrt to their arguments. The* k_i^z, k_i^ψ, k_i^x *and* k_i^y *are positive and stable coefficients. 'd' denotes the desired trajectory.*

Proof. Details of the proof are given in [10].

11.5.2 Bidirectional X4-flyer

Recall that the two rotors 1-3 can be directed together or differently leading to a longitudinal/lateral force. This force contributes to the displacement of the vehicle along the x/y axis, and is denoted by u_2. To bring the engine from one axis to another or both of them, one generates yaw motions first. As we can see in the following, the singularity occurs when $\psi = \pm\frac{\pi}{2}$. In order to avoid the singularity, u_2 should change structure. The static feedback linearization and feed-forward techniques are combined to ensure tracking.

Our first interest is the dynamics of (y,z), which can be decoupled by a static feedback law if the decoupling matrix is not singular. Then we have the following proposition.

Proposition 1. *Consider* $(\psi, \theta) \in]-\pi/2, \pi/2[$, *with the static feedback laws*

$$\begin{aligned} u_2 &= m\nu_y C_\phi C_\psi^{-1} - m(\nu_z + g) S_\phi C_\psi^{-1}, \\ u_3 &= m\nu_y (S_\phi C_\theta^{-1} - C_\phi t g_\psi t g_\theta) + m(\nu_z + g)(C_\phi C_\theta^{-1} + S_\phi t g_\psi t g_\theta) \end{aligned} \tag{11.19}$$

and

$$\begin{aligned} \nu_y &= \ddot{y}_r - k_y^1(\dot{y} - \dot{y}_r) - k_y^2(y - y_r), \\ \nu_z &= \ddot{z}_r - k_z^1(\dot{z} - \dot{z}_r) - k_z^2(z - z_r). \end{aligned} \tag{11.20}$$

The dynamics of y *and* z *are linearly decoupled and exponentially stable with the appropriate choice of the gain controller* k_y^i *and* k_z^i.

Proof. From (11.15), one regroups the two dynamics as

$$\begin{pmatrix} \ddot{y} \\ \ddot{z} \end{pmatrix} = \frac{1}{m} \begin{pmatrix} S_\theta S_\psi S_\phi + C_\psi C_\phi & C_\theta S_\phi \\ S_\theta S_\psi C_\phi - C_\psi S_\phi & C_\theta C_\phi \end{pmatrix} \begin{pmatrix} u_2 \\ u_3 \end{pmatrix} - \begin{pmatrix} 0 \\ g \end{pmatrix}. \tag{11.21}$$

When incorporating inputs (11.19) in system (11.21), we get

$$\ddot{y} = \nu_y, \qquad \ddot{z} = \nu_z. \tag{11.22}$$

Taking θ close to zero, a feed-forward form of the x dynamic is given by

$$\ddot{x} = \frac{1}{m}(S_\psi u_2 - \theta u_3), \qquad \ddot{\theta} = \tilde{\tau}_\theta \tag{11.23}$$

while u_2 and u_3 were already defined in Proposition 1. Note that the dynamics of x seems to be a *zero dynamics*, but it is connected to θ, which is in its turn connected to $\tilde{\tau}_\theta$.

Proposition 2. *Suppose there exists a time* T_f^1 *such that* $\forall t \in [T_0, T_f^1]$ $u_3(t) > 0$. *Then the dynamics of* x *is decoupled under the following feedback controller*

$$\tilde{\tau}_\theta = \frac{1}{u_3}(-m\nu_x + \ddot{\psi} C_\psi u_2 - \dot{\psi}^2 S_\psi u_2 + 2\dot{\psi} C_\psi \dot{u}_2 + S_\psi \ddot{u}_2 - 2\dot{\theta}\dot{u}_3 - \theta \ddot{u}_3) \tag{11.24}$$

leading to $x^{(4)} = \nu_x$ *with*

$$\nu_x = x_d^{(4)} - k_x^1(x^{(3)} - x_d^{(3)}) - k_x^2(\ddot{x} - \ddot{x}_d) - k_x^3(\dot{x} - \dot{x}_d) - k_x^4(x - x_d) \tag{11.25}$$

which stabilizes the system exponentially ($x = x_d, \theta = 0$). k_x^i *are stable coefficients.*

This last result is straightforward and can be shown after having derived twice the dynamics of x. Note that $u_3 > 0$ and $u_3 = mg \; \forall t > T_f^1$, then the drone reaches the desired equilibrium ($x \to x_d, \theta \to \frac{-\ddot{x}}{g} \to 0$). The drawback of the controller (11.24) is that it requires the first/second time derivative of u_3. Then a smooth reference trajectory is required. Moreover, and in order to reduce the calculation complexity of the controller, we can replace in (11.24) $\psi, \dot{\psi}, \ddot{\psi}$ by the references $\psi_d, \dot{\psi}_d, \ddot{\psi}_d$. In fact, ψ can be stabilized separately and reaches $\psi_d \in]-\pi/2, \pi/2[$.

Remark 3. The interval limit of $\psi_d \in]-\pi/2, \pi/2[$ is a handicap for the machine if one wants a displacement according to x with the force input u_2. In this case, the displacement along x requires an orientation of $\psi_d = \pi/2$, which is a singularity for u_2 (see (11.19)). We give a solution to this problem in the following.

Our second interest is the (x, z) dynamics, which can be also decoupled by a static feedback law as shown in the following proposition. Therefore, we keep the input u_3 for the altitude z stabilization and u_2 for the dynamics of x.

Proposition 3. *With the new inputs*

$$\begin{aligned} u_2 &= (S_\psi C_\phi - S_\theta C_\psi S_\phi)^{-1}(m\nu_x C_\phi C_\theta + m(\nu_z + g)S_\theta), \\ u_3 &= (S_\psi C_\phi - S_\theta C_\psi S_\phi)^{-1}(-m\nu_x(S_\psi S_\theta C_\phi - C_\psi S_\phi) + m(\nu_z + g)S_\psi C_\theta) \end{aligned} \tag{11.26}$$

leading to

$$\ddot{x} = \nu_x, \qquad \ddot{z} = \nu_z, \tag{11.27}$$

the dynamics of x and z can be decoupled and stabilized through ν_x and ν_z as above.

Remark 4. The control inputs u_2 and u_3 in Proposition 3 ensure the tracking control in the $x - z$ plane. Further, one needs to stabilize the y motion. The problem can be formulated as in (11.23), where ϕ can be chosen as an input variable. The dynamics of y coupled to ϕ is in cascade form. Consequently $\tilde{\tau}_\phi$ can be deduced with the same procedure given in (11.24).

Remark 5. To switch between the two controllers (11.19) and (11.26) continuity is recommended which permits to avoid the peak phenomenon. This can be asserted if we impose constraints to the reference trajectories. In order to ensure this, we take $u_2(\psi = 0) = u_2(\psi = \pi/2) = 0$ with $\phi = \theta = 0$. For $\psi = 0$ one uses (11.19) and for $\psi = \pi/2$, one refers to expression (11.26). Then from (11.19), (11.26) we deduce that $\nu_y(T_f^2) = \nu_x(T_f^2)$ and $\ddot{y}_d(T_f^2) = \ddot{x}_d(T_f^2)$. Taking $\phi = \theta = 0$, we impose that $u_3(\psi = 0) = mg$ in Eq. (11.19) and $u_3(\psi = \pi/2) = mg$ in Eq. (11.26). T_f^2 is the necessary final time to reach $x_d(T_f^2)$.

11.6 Motion Planning and Simulation Results

In order to validate the motion planning algorithm with the proposed controller, the conventional and bidirectional X4-flyer are tested in simulation. The total mass of the drone is $m = 2$ kg. The technical characteristics of this flying vehicle were presented in [10]. We have considered the following reference trajectory

$$z_d(t) = h_d \frac{t^5}{t^5 + (T_f^1 - t)^5}, \tag{11.28}$$

where h_d is the desired altitude and T_f^1 is the necessary final time. The same trajectory is adopted for $x_d(t)$ and $y_d(t)$. The constraints to perform these trajectories and to ensure continuity in the proposed control schemes are such that $z_d(0) = x_d(T_f^1) = y_d(T_f^2) = 0$, $z_d(T_f^1) = h_d$, $\dot{z}_d(0) = \dot{x}_d(T_f^1) = \dot{y}_d(T_f^2) = 0$, $\dot{z}_d(T_f^1) = \dot{x}_d(T_f^2) = \dot{y}_d(T_f^3) = 0$, $\ddot{z}_d(T_f^1) = \ddot{x}_d(T_f^2) = \ddot{y}_d(T_f^3) = 0$, $\ddot{z}_d(0) = \ddot{x}_d(T_f^1) = \ddot{y}_d(T_f^2) = 0$. T_f^2 and T_f^3 are the final times to execute motion along x and y, respectively. Minimizing the time of displacement here implies that the drone accelerates at the beginning and decelerates at the arrival.

We connect the reference $z - x$ as in Fig. 11.7, considering

$$x_d(t) = -\rho\cos(\alpha(t)) + \rho \qquad \text{and} \qquad z_d(t) = \rho\sin(\alpha(t)) + h_d \tag{11.29}$$

and for the reference transition $x - y$, we take

$$x_d(t) = \rho \sin(\alpha(t)) + x_d(T_f^2) \qquad \text{and} \qquad y_d(t) = -\rho \cos(\alpha(t)) + \rho. \tag{11.30}$$

To ensure continuity between $x_d(t)$ and $y_d(t)$ derivatives, we take

$$\alpha(t) = \frac{\alpha_d (t - t_f)^5}{(t - t_f)^5 + (t_a - t)^5}, \tag{11.31}$$

where $\rho = 2$ m, $\alpha_d = k_\alpha \pi/2$ $(k_\alpha = 1, 2)$, $t_a = 6$ s, $t_f = 8$ s, $x_d(T_f^2) = y_d(T_f^3) = h_d + \rho = 10$ m.

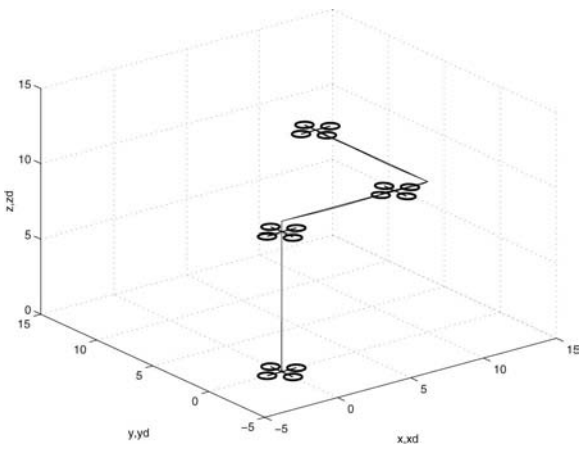

Fig. 11.5. xyz-flying path: conventional X4-flyer

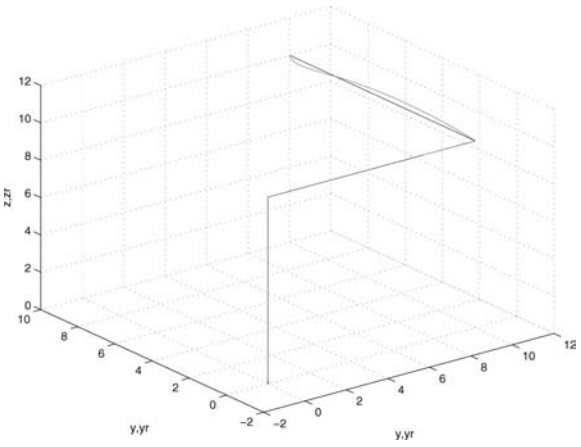

Fig. 11.6. xyz-flying path: bidirectional X4 flyer

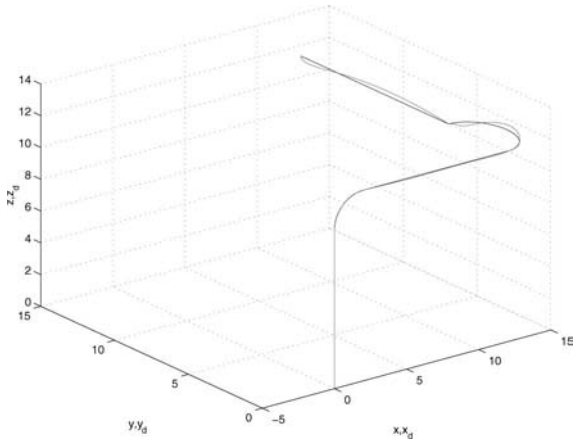

Fig. 11.7. Bidirectional xyz-flying path realization

Figures 11.5-11.6 show a flying path with straight corners: the conventional case result is sketched in Fig. 11.5, and the bidirectional behavior is shown in Fig. 11.6. The engine is maintained horizontal ($\theta = \phi = 0$) (Fig. 11.5), meaning that u_2 is used to perform the longitudinal/lateral displacements. The difference between the two realizations is not notable. The performance of the proposed control laws with the bidirectional flying machine is shown in Fig. 11.7.

11.7 Conclusions

We have considered in this work the modeling and stabilizing/tracking control problem for the three decoupled displacements of a conventional and bidirectional X4-flyer machine. The objectives were to test the capability of engines to fly with rounded intersections and crossroads. The two internal degrees of freedom lead to a longitudinal/lateral force which permits to steer the system with rounded corner flying path. The proposed control inputs permit to perform the tracking objectives: flying path with straight and round corners like connection.

References

1. M. Fliess, J. Levine, P. Martin, P. Rouchon. Flatness and defect of nonlinear systems: introductory theory and examples. *Int. J. of Control*, vol. 61, no. 6, 1995, pp. 1327-1361.
2. P. Martin, R.M. Murray, P. Rouchon. *Flat systems, equivalence and trajectory generation.* Technical report, Ecole des Mines de Paris, April 2003.
3. E. Altug, J. Ostrowski, R. Mahony. Control of a quadrotor helicopter using visual feedback. In: *Proc. IEEE Conf. on Robotics and Automation*, Washington, DC 2002, pp. 72-77.

4. P. Pound, R. Mahony, P. Hynes, J. Roberts. Design of a four rotor aerial robot. *Proc. of the Australasian Conf. on Robotics and Automation*, Auckland 2002.
5. T. Hamel, R. Mahony, R. Lozano, J. Ostrowski. Dynamic modelling and configuration stabilization for an X4-flyer. In: *Proc. IFAC 15th World Congress on Automatic Control*, Barcelona 2002.
6. P. Castillo, A. Dzul, R. Lozano. Real-time stabilization and tracking of a four rotor mini-rotorcraft. *IEEE Trans. on Control Systems Technology*, vol. 12, no. 4, 2004, pp. 510-516.
7. J. Hauser, S. Sastry, G. Meyer. Nonlinear control design for slightly non minimum phase systems: application to V/STOL aircraft. *Automatica*, vol. 28, no. 4, 1992, pp. 665-679.
8. L. Marconi, A. Isodori. Robust output regulation for autonomous vertical landing. In: *Proc. 39th IEEE Conf. on Decision and Control*, Sydney 2000.
9. B.W. McCormick, Jr. *Aerodynamics of V/STOL flight.* Academic Press, New York 1967.
10. L. Beji, A. Abichou. Streamlined rotors mini rotorcraft: trajectory generation and tracking. *Int. J. of Control, Automation, and Systems*, vol. 3, no. 1, 2005, pp. 87-99.
11. L. Beji, A. Abichou, M.K. Zemalache. Smooth control of an X4 bidirectional rotors flying robot. In: *Proc. IEEE Int. Workshop on Robot Motion and Control (RoMoCo)*, Dymaczewo, Poland 2005.